

Ω baryon spectrum and their decays in a constituent quark model

Ming-Sheng Liu,^{1,2,3,*} Kai-Lei Wang,^{2,4,†} Qi-Fang Lü^{‡,1,2,3,§} and Xian-Hui Zhong^{¶1,2,3,**}

¹ Department of Physics, Hunan Normal University, Changsha 410081, China

² Synergetic Innovation Center for Quantum Effects and Applications (SICQEA), Changsha 410081, China

³ Key Laboratory of Low-Dimensional Quantum Structures and Quantum Control of Ministry of Education, Changsha 410081, China

⁴ Department of Electronic Information and Physics, Changzhi University, Changzhi, Shanxi, 046011, China

Combining the recent developments of the observations of Ω sates we calculate the Ω spectrum up to the $N = 2$ shell within a nonrelativistic constituent quark potential model. Furthermore, the strong and radiative decay properties for the Ω resonances within the $N = 2$ shell are evaluated by using the masses and wave functions obtained from the potential model. It is found that the newly observed $\Omega(2012)$ resonance is most likely to be the spin-parity $J^P = 3/2^-$ $1P$ -wave state $\Omega(1^2P_{3/2^-})$, it also has a large potential to be observed in the $\Omega(1672)\gamma$ channel. Our calculation shows that the $1P$ -, $1D$ -, and $2S$ -wave Ω baryons have a relatively narrow decay width of less than 50 MeV. Based on the obtained decay properties and mass spectrum, we further suggest optimum channels and mass regions to find the missing Ω resonances via the strong and/or radiative decay processes.

PACS numbers:

Keywords:

I. INTRODUCTION

Searching for the missing baryon resonances and understanding the baryon spectrum are important topics in hadron physics. Our knowledge about the Ω hyperon spectrum is very poor compared with the other light baryon spectra. Only a few data on the Ω resonances have been reported in experiments since the discovery of the ground state $\Omega(1672)$ at BNL in 1964 [1]. Before 2018, except for the ground state $\Omega(1672)$ only three Ω resonances $\Omega(2250)$, $\Omega(2380)$ and $\Omega(2470)$ were listed in the Review of Particle Physics (RPP) [2]. Due to the slow development in experiments, most of the theoretical studies are limited in the calculations of the mass spectrum of the Ω baryon with various methods, such as the Skyrme model [3], the relativistic quark models [4–6], the nonrelativistic quark model [7–12], the lattice gauge theory [13, 14], and so on.

Fortunately, the Belle II experiments can offer a great opportunity for our study of the Ω spectrum. In 2018, the Belle Collaboration reported a new resonance denoted by $\Omega(2012)$ [15], a candidate of excited Ω state decaying into $\Xi^0 K^-$ and $\Xi^- K_s^0$ with a mass of

$$M = 2012.4 \pm 0.7(\text{stat.}) \pm 0.6(\text{syst.}) \text{ MeV},$$

and a width of

$$\Gamma = 6.4_{-2.0}^{+2.5}(\text{stat.}) \pm 0.6(\text{syst.}) \text{ MeV}.$$

According to the calculations of the Ω mass spectrum in the various models [4–12], the $\Omega(2012)$ resonance may be a good

candidate for the first orbital excitations of Ω baryon. Stimulated by the newly observed $\Omega(2012)$, by using a simple harmonic oscillator (SHO) wave functions, the strong decay properties of the Ω spectrum up to the $N = 2$ shell were studied within the chiral quark model [16] and quark pair creation model [17], respectively. The results show that $\Omega(2012)$ could be assigned to the spin-parity $J^P = 3/2^-$ $1P$ -wave Ω state, which is supported by the QCD Sum rule analysis in Refs. [18, 19], and the flavor SU(3) analysis in Ref. [20]. There also exist other interpretations, such as hadronic molecule state, of the newly observed $\Omega(2012)$ state in the literature. Considering the mass of $\Omega(2012)$ is very close to $\Xi(1530)K$ threshold, the authors in Refs. [21–23] interpreted $\Omega(2012)$ as the S -wave $\Xi(1530)K$ hadronic molecule state with quantum number $J^P = 3/2^-$. In the Ref. [24], $\Omega(2012)$ is assumed to be a dynamically generated state with spin parity $J^P = 3/2^-$ from the coupled channel S -wave interactions of $\bar{K}\Xi(1530)$ and $\eta\Omega$. Very recently, the Belle Collaboration searched for the three-body decay of the $\Omega(2012)$ baryon to $K\pi\Xi$ [25]. No significant $\Omega(2012)$ signals have been observed in the studied channels. The experimental result strongly disfavors the molecular interpretation [25].

In this work, we further study the Ω spectrum. First, combining the recent developments of the observations of Ω sates in experiments at Belle we calculate the mass spectrum up to the $N = 2$ shell within a nonrelativistic constituent quark potential model. Then, by using the masses and wave functions calculated from the potential model, we give our predictions of the strong and radiative decay properties for the Ω resonances. The strong decay properties for the P - and D -wave states predicted with the realistic wave functions of the potential model are compatible with the results obtained with the SHO wave functions in Ref. [16]. The strong decays of the $2S$ -wave states show some sensitivities to the details of the wave functions, the strong decay properties of these $2S$ -wave states predicted in present work have some differences from those calculated with the SHO wave functions. The $\Omega(2012)$ resonance is most likely to be the spin-parity $J^P = 3/2^-$ $1P$ -

*Corresponding author

¶Corresponding author

*Electronic address: liumingsheng0001@126.com

†Electronic address: wangkaileicz@foxmail.com

§Electronic address: lvqifang@hunnu.edu.cn

**Electronic address: zhongxh@hunnu.edu.cn

wave state $\Omega(1^2P_{3/2^-})$. Both the mass and decay properties predicted in theory are consistent with the observations. The $\Omega(2012)$ state may be observed in the radiative decay channel $\Omega(1672)\gamma$ as well. Furthermore, based on the obtained decay properties and mass spectrum, we suggest optimum channels and mass regions to find the missing $1P^-$, $1D^-$, and $2S^-$ -wave Ω resonances in the strong and/or radiative decay processes.

This paper is organized as follows. In Sec. II, we study the mass spectrum of the Ω baryon in the nonrelativistic constituent quark potential model. Then, in Sec. III, we give a review of the decay models, and calculate the strong and radiative decays of the excited Ω states by using the masses and wave functions obtained from the potential model. In Sec. IV, we give our discussions based on the obtained decay properties and masses of the Ω resonances. Finally, a summary is given in Sec. V.

II. MASS SPECTRUM

A. Hamiltonian

To calculate the spectrum of the Ω baryon, we adopt the following nonrelativistic Hamiltonian

$$H = \left(\sum_{i=1}^3 m_i + T_i \right) - T_G + \sum_{i<j} V_{ij}(r_{ij}) + C_0, \quad (1)$$

where m_i and T_i stand for the constituent quark mass and kinetic energy of the i -th quark, respectively; T_G stands for the center-of-mass (c.m.) kinetic energy of the baryon system; $r_{ij} \equiv |\mathbf{r}_i - \mathbf{r}_j|$ is the distance between the i -th quark and j -th quark; zero point energy C_0 is a constant, and $V_{ij}(r_{ij})$ stands for the effective potential between the i -th and j -th quark. In this work, we adopt a widely used potential form for $V_{ij}(r_{ij})$ [26–35], i.e.

$$V_{ij}(r_{ij}) = V_{ij}^{conf}(r_{ij}) + V_{ij}^{sd}(r_{ij}), \quad (2)$$

where V_{ij}^{conf} stands for the potential for confinement, and is adopted the standard Coulomb+linear scalar form:

$$V_{ij}^{conf}(r_{ij}) = \frac{b}{2}r_{ij} - \frac{2\alpha_s}{3r_{ij}}, \quad (3)$$

while $V_{ij}^{sd}(r_{ij})$ stands for the spin-dependent interaction, which is the sum of the spin-spin contact hyperfine potential V_{ij}^{SS} , the tensor term V_{ij}^T , and the spin-orbit term V_{ij}^{LS}

$$V_{ij}^{sd} = V_{ij}^{SS} + V_{ij}^T + V_{ij}^{LS}. \quad (4)$$

The spin-spin potential V_{ij}^{SS} and the tensor term V_{ij}^T are adopted the often used forms:

$$V_{ij}^{SS} = -\frac{2\alpha_s}{3} \left\{ -\frac{\pi}{2} \cdot \frac{\sigma_{ij}^3 e^{-\sigma_{ij}^2 r_{ij}^2}}{\pi^{3/2}} \cdot \frac{16}{3m_i m_j} (\mathbf{S}_i \cdot \mathbf{S}_j) \right\}, \quad (5)$$

$$V_{ij}^T = \frac{2\alpha_s}{3} \cdot \frac{1}{m_i m_j r_{ij}^3} \left\{ \frac{3(\mathbf{S}_i \cdot \mathbf{r}_{ij})(\mathbf{S}_j \cdot \mathbf{r}_{ij})}{r_{ij}^2} - \mathbf{S}_i \cdot \mathbf{S}_j \right\}. \quad (6)$$

In this work, a simplified phenomenological spin-orbit potential is adopted the same form as that suggested in the literature [12, 36], i.e.,

$$V_{ij}^{LS} = \frac{\alpha_{SO}}{\rho^2 + \lambda^2} \cdot \frac{\mathbf{L} \cdot \mathbf{S}}{3(m_1 + m_2 + m_3)^2}. \quad (7)$$

In the above equations, the parameter b denotes the strength of the confinement potential. The \mathbf{S}_i , \mathbf{S} and \mathbf{L} are the spin operator of the i -th quark, the total spin of the baryon and the total orbital angular momentum of the baryon, respectively.

B. Wave functions in the SU(6)×O(3) symmetry limit

The total wave function of a baryon system should include four parts: a color wave function ζ , a flavor wave function ϕ , a spin wave function χ , and a spatial wave function ψ . The color wave function ζ should be a color singlet under SU(3) symmetry, one can explicitly express it as

$$\zeta = \frac{1}{\sqrt{6}}(rgb - rbg + gbr - grb + brg - bgr). \quad (8)$$

For a light baryon system, the flavor wave function ϕ and the spin wave function χ together form an SU(6) symmetry. The SU(6) spin-flavor wave functions can be found in the literature [37]. Without a spin-dependent interaction in the Hamiltonian for three-body systems, the total orbital angular momentum \mathbf{L} and the total spin \mathbf{S} are conserved. The total angular momentum of the baryon is $\mathbf{J} = \mathbf{L} + \mathbf{S}$, and thus the spatial wave functions possess O(3) symmetry under a rotation transformation. Meanwhile, the Hamiltonian for a three-quark system can be invariant under the permutation group S_3 . One thus can express the spatial wave functions as representations of the S_3 group. To consider the S_3 symmetry, one can express the three coordinates \mathbf{r}_1 , \mathbf{r}_2 , and \mathbf{r}_3 with the Jacobi coordinates \mathbf{R} , $\boldsymbol{\rho}$ and $\boldsymbol{\lambda}$ by the following transformation,

$$\boldsymbol{\rho} \equiv \frac{1}{\sqrt{2}}(\mathbf{r}_1 - \mathbf{r}_2), \quad (9)$$

$$\boldsymbol{\lambda} \equiv \sqrt{\frac{2}{3}} \left(\frac{m_1 \mathbf{r}_1 + m_2 \mathbf{r}_2}{m_1 + m_2} - \mathbf{r}_3 \right), \quad (10)$$

$$\mathbf{R} \equiv \frac{\sqrt{3}(m_1 \mathbf{r}_1 + m_2 \mathbf{r}_2 + m_3 \mathbf{r}_3)}{m_1 + m_2 + m_3}. \quad (11)$$

The symmetric coordinate \mathbf{R} describes the usual center of mass motion, and two mixed coordinates $\boldsymbol{\rho}$ and $\boldsymbol{\lambda}$ describe the internal motions which are antisymmetric and symmetric under the exchange of quark 1 and 2. The corresponding spatial wave function ψ may be generally written as

$$\psi(\mathbf{r}_1, \mathbf{r}_2, \mathbf{r}_3) = e^{i\mathbf{P}_R \cdot \mathbf{R}} \psi_{NLM_L}^\sigma(\boldsymbol{\rho}, \boldsymbol{\lambda}) \quad (12)$$

where $\psi_{NLM_L}^\sigma(\boldsymbol{\rho}, \boldsymbol{\lambda})$ is the spatial wave function, which can be determined by solving the Schrödinger equation; $\sigma = s, \rho, \lambda$, a denotes the representation of the S_3 group.

TABLE I: The masses (MeV) of Ω baryons with principal quantum number $N \leq 2$. For comparison, the experimental measured masses [2, 15] and the theory predictions [3, 5–8, 12, 13] are also listed. Recently, the quantum number of the resonances $\Omega(2012)$ [15] and $\Omega(2250)$ [2] are not determined. According the Ref. [16, 17], we think the resonances $\Omega(2012)$ and $\Omega(2250)$ as state $\Omega(1^2P_{3/2^-})$ and state $\Omega(1^4D_{5/2^+})$, respectively.

$n^{2S+1}L_J P$	$ N_6, {}^{2S+1}N_3, N, L, J^P\rangle$	Ours	Exp.	Ref. [3]	Ref. [5]	Ref. [6]	Ref. [7]	Ref. [8]	Ref. [12]	Ref. [13]
$1^4S_{\frac{3}{2}^+}$	$ 56, {}^4 10, 0, 0, \frac{3}{2}^+\rangle$	1672	1672.45 [2]	1694	1635	1678	1675	1673	1656	1642(17)
$1^2P_{\frac{1}{2}^-}$	$ 70, {}^2 10, 1, 1, \frac{1}{2}^-\rangle$	1957	...	1837	1950	1941	2020	2015	1923	1944(56)
$1^2P_{\frac{3}{2}^-}$	$ 70, {}^2 10, 1, 1, \frac{3}{2}^-\rangle$	2012	2012.4 [15]	1978	2000	2038	2020	2015	1953	2049(32)
$2^2S_{\frac{1}{2}^+}$	$ 70, {}^2 10, 2, 0, \frac{1}{2}^+\rangle$	2232	...	2140	2220	2301	2190	2182	2191	2350(63)
$2^4S_{\frac{3}{2}^+}$	$ 56, {}^4 10, 2, 0, \frac{3}{2}^+\rangle$	2159	2165	2173	2065	2078	2170	...
$1^2D_{\frac{3}{2}^+}$	$ 70, {}^2 10, 2, 2, \frac{3}{2}^+\rangle$	2245	...	2282	2345	2304	2265	2263	2194	2470(49)
$1^2D_{\frac{5}{2}^+}$	$ 70, {}^2 10, 2, 2, \frac{5}{2}^+\rangle$	2303	2345	2401	2265	2260	2210	...
$1^4D_{\frac{1}{2}^+}$	$ 56, {}^4 10, 2, 2, \frac{1}{2}^+\rangle$	2141	...	2140	2255	2301	2210	2202	2175	2481(51)
$1^4D_{\frac{3}{2}^+}$	$ 56, {}^4 10, 2, 2, \frac{3}{2}^+\rangle$	2188	...	2282	2280	2304	2215	2208	2182	2470(49)
$1^4D_{\frac{5}{2}^+}$	$ 56, {}^4 10, 2, 2, \frac{5}{2}^+\rangle$	2252	2252 [2]	...	2280	2401	2225	2224	2178	...
$1^4D_{\frac{7}{2}^+}$	$ 56, {}^4 10, 2, 2, \frac{7}{2}^+\rangle$	2321	2295	2332	2210	2205	2183	...

The states in the $SU(6) \times O(3)$ representation up to $N = 2$ shell are given in Table I. We denote the baryon states as $|N_6, {}^{2S+1}N_3, N, L, J^P\rangle$, where N_6 stands for the irreducible representation of spin-flavor $SU(6)$ group, N_3 stands for the irreducible representation of flavor $SU(3)$ group, and N, S, L , and J^P stand for the principal, spin, total orbital angular momentum, and spin-parity quantum numbers, respectively. More details about the $SU(6) \times O(3)$ wave functions can be found in Ref. [37].

C. Numerical calculation

1. Trial spatial wave functions

To obtain spatial wave functions and the masses for every Ω states in the $SU(6) \times O(3)$ representation, one need solve the Schrödinger equation. The spatial wave function $\psi_{NLM_L}^\sigma(\boldsymbol{\rho}, \boldsymbol{\lambda})$ may be expressed as the linear combination of $\psi_{n_\rho l_\rho m_\rho}(\boldsymbol{\rho})\psi_{n_\lambda l_\lambda m_\lambda}(\boldsymbol{\lambda})$:

$$\psi_{NLM_L}^\sigma(\boldsymbol{\rho}, \boldsymbol{\lambda}) = \sum_{\substack{N=2(n_\rho+n_\lambda) \\ +l_\rho+l_\lambda \\ M_L=m_\rho+m_\lambda}} C_{n_\lambda l_\lambda m_\lambda}^{n_\rho l_\rho m_\rho} [\psi_{n_\rho l_\rho m_\rho}(\boldsymbol{\rho})\psi_{n_\lambda l_\lambda m_\lambda}(\boldsymbol{\lambda})]_{NLM_L}^\sigma \quad (13)$$

The ρ - and λ -mode spatial wave functions $\psi_{n_\rho l_\rho m_\rho}(\boldsymbol{\rho})$ and $\psi_{n_\lambda l_\lambda m_\lambda}(\boldsymbol{\lambda})$ can be written with a unified form:

$$\psi_{n_\ell l_\ell m_\ell}(\boldsymbol{\xi}) = R_{n_\ell l_\ell}(\xi) Y_{l_\ell m_\ell}(\hat{\boldsymbol{\xi}}), \quad (14)$$

where the $Y_{l_\ell m_\ell}(\hat{\boldsymbol{\xi}})$ is the spherical harmonic function. In the above equations, l_ρ and l_λ are the quantum numbers of the relative orbital angular momenta \mathbf{l}_ρ and \mathbf{l}_λ of the ρ - and λ -mode oscillators, respectively, while L is the quantum number of the total momentum $\mathbf{L} = \mathbf{l}_\lambda + \mathbf{l}_\rho$ for the system. The n_ρ and n_λ are the principal quantum numbers of the ρ - and λ -mode oscillators, respectively, and $N = 2n_\rho + 2n_\lambda + l_\rho + l_\lambda$.

The coefficients $C_{n_\lambda l_\lambda m_\lambda}^{n_\rho l_\rho m_\rho}$ and explicit forms of the spatial wave function $\psi_{NLM_L}^\sigma(\boldsymbol{\rho}, \boldsymbol{\lambda})$ up to the $N = 2$ shell have been given in Table II.

The radial wave function $R_{n_\ell l_\ell}(\xi)$ is adopted a trial form by expanding with a series of harmonic oscillator functions:

$$R_{n_\ell l_\ell}(\xi) = \sum_{\ell=1}^n C_{\ell l_\ell} \phi_{n_\ell l_\ell}(d_{\ell l_\ell}, \xi), \quad (15)$$

where

$$\begin{aligned} \phi_{n_\ell l_\ell}(d_{\ell l_\ell}, \xi) &= \left(\frac{1}{d_{\ell l_\ell}}\right)^{\frac{3}{2}} \left[\frac{2^{l_\ell+2-n_\ell} (2l_\ell+2n_\ell+1)!!}{\sqrt{\pi n_\ell} [(2l_\ell+1)!!]^2} \right]^{\frac{1}{2}} \left(\frac{\xi}{d_{\ell l_\ell}}\right)^{l_\ell} \\ &\times e^{-\frac{1}{2} \left(\frac{\xi}{d_{\ell l_\ell}}\right)^2} F\left(-n_\ell, l_\ell + \frac{3}{2}, \left(\frac{\xi}{d_{\ell l_\ell}}\right)^2\right). \end{aligned} \quad (16)$$

The $F\left(-n_\ell, l_\ell + \frac{3}{2}, \left(\frac{\xi}{d_{\ell l_\ell}}\right)^2\right)$ is the confluent hypergeometric function. The parameter $d_{\ell l_\ell}$ can be related to the harmonic oscillator frequency $\omega_{\ell l_\ell}$ with $1/d_{\ell l_\ell}^2 = M_\xi \omega_{\ell l_\ell}$. The reduced masses $M_{\rho, \lambda}$ are defined by $M_\rho \equiv \frac{2m_1 m_2}{m_1 + m_2}$, $M_\lambda \equiv \frac{3(m_1 + m_2)m_3}{2(m_1 + m_2 + m_3)}$. On the other hand, the harmonic oscillator frequency $\omega_{\ell l_\ell}$ can be related to the harmonic oscillator stiffness factor K_ℓ with $\omega_{\ell l_\ell} = \sqrt{3K_\ell/M_\xi}$ [37]. For a sss system, one has $d_{\rho\ell} = d_{\lambda\ell} = d_\ell = (3m_s K_\ell)^{-1/4}$, where m_s stands for the constituent mass of the strange quark. With this relation, the spatial wave function $\psi_{NLM_L}^\sigma(\boldsymbol{\rho}, \boldsymbol{\lambda})$ can be simply expanded as

$$\psi_{NLM_L}^\sigma(\boldsymbol{\rho}, \boldsymbol{\lambda}) = \sum_{\ell} C_{\ell} \psi_{NLM_L}^\sigma(d_\ell, \boldsymbol{\rho}, \boldsymbol{\lambda}), \quad (17)$$

where $\psi_{NLM_L}^\sigma(d_\ell, \boldsymbol{\rho}, \boldsymbol{\lambda})$ stands for the trial harmonic oscillator functions,

$$\begin{aligned} \psi_{NLM_L}^\sigma(d_\ell, \boldsymbol{\rho}, \boldsymbol{\lambda}) &= \sum_{\substack{N=2n_\rho+2n_\lambda+l_\rho+l_\lambda \\ M_L=m_\rho+m_\lambda}} C_{n_\lambda l_\lambda m_\lambda}^{n_\rho l_\rho m_\rho} \\ &[\phi_{n_\rho l_\rho}(d_\ell, \boldsymbol{\rho})\phi_{n_\lambda l_\lambda}(d_\ell, \boldsymbol{\lambda})Y_{l_\rho m_\rho}(\hat{\boldsymbol{\rho}})Y_{l_\lambda m_\lambda}(\hat{\boldsymbol{\lambda}})]_{NLM_L}^\sigma. \end{aligned} \quad (18)$$

2. Matrix elements

The problem of solving the Schrödinger equation is now reduced to one of calculating the matrix elements $H_{\alpha\alpha} = \langle \alpha | H | \alpha \rangle$, where $|\alpha\rangle$ stands for the total wave function $|N_6, {}^{2S+1}N_3, N, L, J^P\rangle$ for the Ω baryons. Omitting the color and flavor wave functions, the total wave function $|\alpha\rangle$ in the $L-S$ coupling scheme can be expressed as

$$|\alpha\rangle = \sum_{M_S+M_L=M} \langle LM_L; SM_S | JM \rangle \psi_{NLM_L}^\sigma(\boldsymbol{\rho}, \boldsymbol{\lambda}) \chi_{M_S}^\sigma. \quad (19)$$

With the Jacobi coordinates $\boldsymbol{\rho}$ and $\boldsymbol{\lambda}$, the matrix elements $H_{\alpha\alpha}$ can be expressed as

$$H_{\alpha\alpha} = 3m_s + C_0 + \left\langle \alpha \left| \frac{p_\rho^2}{2m_\rho} + \frac{p_\lambda^2}{2m_\lambda} \right| \alpha \right\rangle + \left\langle \alpha \left| \sum_{i<j} V_{ij}(r_{ij}) \right| \alpha \right\rangle, \quad (20)$$

where $r_{12} = \sqrt{2}\rho$, $r_{13} = \sqrt{(\rho^2 + \sqrt{3}\boldsymbol{\rho} \cdot \boldsymbol{\lambda} + 3\lambda^2)/2}$, $r_{23} = \sqrt{(\rho^2 - \sqrt{3}\boldsymbol{\rho} \cdot \boldsymbol{\lambda} + 3\lambda^2)/2}$. Replacing $p_{\xi=\rho,\lambda}^2$ with the operators $-\frac{1}{\xi^2} \frac{\partial}{\partial \xi} (\xi^2 \frac{\partial}{\partial \xi}) + \frac{l(l+1)}{\xi^2}$, the kinetic energy matrix elements $\langle \alpha | \frac{p_\rho^2}{2m_\rho} + \frac{p_\lambda^2}{2m_\lambda} | \alpha \rangle$ in Eq. (20) can be easily worked out in the coordinate space.

Then some calculations of the matrix elements of the potentials between quarks become the main task of present work. Considering the permutation symmetry of the total wave function of the Ω baryons, we can obtain

$$\left\langle \alpha \left| \sum_{i<j} V_{ij}(r_{ij}) \right| \alpha \right\rangle = 3 \langle \alpha | V_{12}(r_{12}) | \alpha \rangle. \quad (21)$$

Finally, we can therefore specialize our discussion to techniques for calculating potential matrix elements of the $V_{12}(r_{12})$ terms.

The matrix elements of confining potential V_{12}^{conf} , and spin-orbit potential V_{12}^{LS} can be directly worked out with the total wave function $|\alpha\rangle$ in the $L-S$ coupling scheme. The calculations of the matrix elements of tensor potential V_{12}^T , and spin-spin potential V_{12}^{SS} , are relatively complicated. We transform $|\alpha\rangle$ into the $|\beta\rangle = |(s_{12}s_3)S, (l_\rho l_\lambda)L, (n_\rho n_\lambda)N, JM\rangle$ representation with the following relation:

$$|\alpha\rangle = \sum_i c_i |\beta\rangle_i. \quad (22)$$

The s_{12} is the quantum number of the spin angular momentum $\mathbf{S}_1 + \mathbf{S}_2$. The coefficients c_i and explicit quantum numbers of the Ω states up to the $N = 2$ shell have been given in Table III. Then with the Wigner-Eckart theorem, the matrix elements of tensor potential V_{12}^T can be worked out with the following form

mula

$$\begin{aligned} & \left\langle \beta' \left| \frac{1}{\rho^3} \left(\frac{3(\mathbf{S}_1 \cdot \boldsymbol{\rho})(\mathbf{S}_2 \cdot \boldsymbol{\rho})}{\rho^2} - \mathbf{S}_1 \cdot \mathbf{S}_2 \right) \right| \beta \right\rangle \\ &= \frac{\sqrt{30}}{2} \times (-1)^{J'+L'+L+l_\lambda+\frac{3}{2}} \times \sqrt{(2l'_\rho+1)(2l_\rho+1)} \\ & \times \sqrt{(2L'+1)(2L+1)(2S'+1)(2S+1)} \\ & \times \begin{Bmatrix} s'_{12} & s'_{12} & 2 \\ S' & S' & \frac{1}{2} \end{Bmatrix} \begin{Bmatrix} S' & L' & J' \\ L' & S' & 2 \end{Bmatrix} \begin{Bmatrix} l'_\rho & l'_\rho & 2 \\ L' & L' & l_\lambda \end{Bmatrix} \begin{Bmatrix} l'_\rho & 2 & l'_\rho \\ 0 & 0 & 0 \end{Bmatrix} \\ & \times \langle \phi_{n'_\rho l'_\rho}(\boldsymbol{\rho}) \phi_{n'_\lambda l'_\lambda}(\boldsymbol{\lambda}) | \rho^{-3} | \phi_{n_\rho l_\rho}(\boldsymbol{\rho}) \phi_{n_\lambda l_\lambda}(\boldsymbol{\lambda}) \rangle \\ & \times \delta_{S'_{12} 1} \delta_{S_{12} 1} \delta_{l'_\lambda l_\lambda} \delta_{J' J} \delta_{M' M}, \end{aligned} \quad (23)$$

and the matrix elements of spin-spin potential V_{12}^{SS} can be worked out with the following formula

$$\begin{aligned} & \left\langle \beta' \left| e^{-\sigma^2 \rho^2} (\mathbf{S}_1 \cdot \mathbf{S}_2) \right| \beta \right\rangle \\ &= \frac{3}{2} \times (-1)^{1+s'_{12}} \times \begin{Bmatrix} \frac{1}{2} & \frac{1}{2} & s'_{12} \\ \frac{1}{2} & \frac{1}{2} & 1 \end{Bmatrix} \delta_{l'_\lambda l_\lambda} \delta_{l'_\rho l_\rho} \delta_{J' J} \delta_{M' M} \\ & \times \langle \phi_{n'_\rho l'_\rho}(\boldsymbol{\rho}) \phi_{n'_\lambda l'_\lambda}(\boldsymbol{\lambda}) | e^{-\sigma^2 \rho^2} | \phi_{n_\rho l_\rho}(\boldsymbol{\rho}) \phi_{n_\lambda l_\lambda}(\boldsymbol{\lambda}) \rangle. \end{aligned} \quad (24)$$

TABLE II: The spatial functions $\psi_{NLM_L}^\sigma(\boldsymbol{\rho}, \boldsymbol{\lambda})$ as the linear combination of $\psi_{n_\rho l_\rho m_\rho}(\boldsymbol{\rho}) \psi_{n_\lambda l_\lambda m_\lambda}(\boldsymbol{\lambda})$.

$\psi_{000}^S(\boldsymbol{\rho}, \boldsymbol{\lambda})$	$= \psi_{000}(\boldsymbol{\rho}) \psi_{000}(\boldsymbol{\lambda})$
$\psi_{11M_L}^\rho(\boldsymbol{\rho}, \boldsymbol{\lambda})$	$= \psi_{01M_L}(\boldsymbol{\rho}) \psi_{000}(\boldsymbol{\lambda})$
$\psi_{11M_L}^\lambda(\boldsymbol{\rho}, \boldsymbol{\lambda})$	$= \psi_{000}(\boldsymbol{\rho}) \psi_{01M_L}(\boldsymbol{\lambda})$
$\psi_{200}^S(\boldsymbol{\rho}, \boldsymbol{\lambda})$	$= \frac{1}{\sqrt{2}} [\psi_{100}(\boldsymbol{\rho}) \psi_{000}(\boldsymbol{\lambda}) + \psi_{000}(\boldsymbol{\rho}) \psi_{100}(\boldsymbol{\lambda})]$
$\psi_{200}^\rho(\boldsymbol{\rho}, \boldsymbol{\lambda})$	$= \frac{1}{\sqrt{2}} [-\psi_{100}(\boldsymbol{\rho}) \psi_{000}(\boldsymbol{\lambda}) + \psi_{000}(\boldsymbol{\rho}) \psi_{100}(\boldsymbol{\lambda})]$
$\psi_{200}^\lambda(\boldsymbol{\rho}, \boldsymbol{\lambda})$	$= \frac{1}{\sqrt{3}} [\psi_{011}(\boldsymbol{\rho}) \psi_{01-1}(\boldsymbol{\lambda}) - \psi_{010}(\boldsymbol{\rho}) \psi_{010}(\boldsymbol{\lambda}) + \psi_{01-1}(\boldsymbol{\rho}) \psi_{011}(\boldsymbol{\lambda})]$
$\psi_{22M_L}^S(\boldsymbol{\rho}, \boldsymbol{\lambda})$	$= \frac{1}{\sqrt{2}} [\psi_{02M_L}(\boldsymbol{\rho}) \psi_{000}(\boldsymbol{\lambda}) + \psi_{000}(\boldsymbol{\rho}) \psi_{02M_L}(\boldsymbol{\lambda})]$
$\psi_{22M_L}^\rho(\boldsymbol{\rho}, \boldsymbol{\lambda})$	$= \frac{1}{\sqrt{2}} [\psi_{02M_L}(\boldsymbol{\rho}) \psi_{000}(\boldsymbol{\lambda}) - \psi_{000}(\boldsymbol{\rho}) \psi_{02M_L}(\boldsymbol{\lambda})]$
$\psi_{222}^\rho(\boldsymbol{\rho}, \boldsymbol{\lambda})$	$= \psi_{011}(\boldsymbol{\rho}) \psi_{011}(\boldsymbol{\lambda})$
$\psi_{221}^\rho(\boldsymbol{\rho}, \boldsymbol{\lambda})$	$= \frac{1}{\sqrt{2}} [\psi_{010}(\boldsymbol{\rho}) \psi_{011}(\boldsymbol{\lambda}) + \psi_{011}(\boldsymbol{\rho}) \psi_{010}(\boldsymbol{\lambda})]$
$\psi_{220}^\rho(\boldsymbol{\rho}, \boldsymbol{\lambda})$	$= \frac{1}{\sqrt{6}} [\psi_{01-1}(\boldsymbol{\rho}) \psi_{011}(\boldsymbol{\lambda}) + 2\psi_{010}(\boldsymbol{\rho}) \psi_{010}(\boldsymbol{\lambda}) + \psi_{011}(\boldsymbol{\rho}) \psi_{01-1}(\boldsymbol{\lambda})]$
$\psi_{22-1}^\rho(\boldsymbol{\rho}, \boldsymbol{\lambda})$	$= \frac{1}{\sqrt{2}} [\psi_{01-1}(\boldsymbol{\rho}) \psi_{010}(\boldsymbol{\lambda}) + \psi_{010}(\boldsymbol{\rho}) \psi_{01-1}(\boldsymbol{\lambda})]$
$\psi_{22-2}^\rho(\boldsymbol{\rho}, \boldsymbol{\lambda})$	$= \psi_{01-1}(\boldsymbol{\rho}) \psi_{01-1}(\boldsymbol{\lambda})$

3. results

In this work, we adopt the variation principle to solve the Schrödinger equation. Following the method used in Refs. [38, 39], the oscillator length d_ℓ are set to be

$$d_\ell = d_1 a^{\ell-1} \quad (\ell = 1, \dots, n), \quad (25)$$

where n is the number of Gaussian functions, and a is the ratio coefficient. There are three parameters $\{d_1, d_n, n\}$ to be determined through variation method. It is found that when

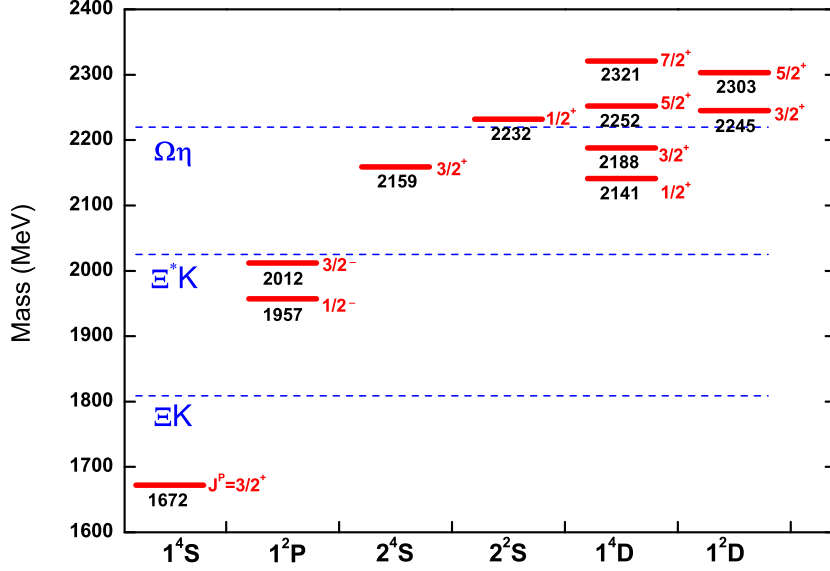


FIG. 1: Mass spectrum of the Ω baryon with principal quantum number $N \leq 2$ (solid lines) and their possible main decay channels (dashed lines). The unit of mass is MeV.

we take $d_1 = 0.085$ fm, $d_n = 3.399$ fm, $n = 15$, we will obtain stable solutions for the Ω baryons.

When all the matrix elements have been worked out, we can solve the generalized matrix eigenvalue problem [39],

$$\sum_{\ell=1}^n \sum_{\ell'=1}^n (H_{\ell\ell'} - E_{\ell} N_{\ell\ell'}) C_{\ell'}^{\ell} = 0, \quad (26)$$

where $H_{\ell\ell'} \equiv \langle \Psi(d_{\ell}') | H | \Psi(d_{\ell}) \rangle$ and $N_{\ell\ell'} \equiv \langle \Psi(d_{\ell}') | \Psi(d_{\ell}) \rangle$. The function $\Psi(d_{\ell})$ is given by

$$\Psi(d_{\ell}) = \sum_{M_L + M_S = M} \langle LM_L, SM_S | JM \rangle \psi_{NLM_L}^{\sigma}(d_{\ell}, \rho, \lambda) \chi_{M_S}^{\sigma}. \quad (27)$$

The physical state corresponds to the solution with a minimum energy E_m . By solving this generalized matrix eigenvalue problem, the masses of the Ω baryons and its spatial wave functions can be determined.

It should be emphasized that there are six parameters m_s , α_s , σ_{ss} , b , α_{SO} and C_0 in the quark potential model. They are determined by fitting the masses of four Ω resonances: (i) The ground state $\Omega(1672)$ [2], which is well established in experiments. (ii) The newly observed $\Omega(2012)$ resonance at Belle [15], which is interpreted as the first orbital excited state $\Omega(1^2P_{3/2^-})$ [16, 17]. (iii) The other first orbital excited state $\Omega(1^2P_{1/2^-})$ whose mass is predicted to be ~ 1950 MeV within the Lattice QCD [13] and the relativized quark models [5, 6]. The measured ΞK invariant mass distributions from Belle show that there is a weak enhancement around 1950 MeV [15], which may be a weak hint of $J^P = 1/2^-$ state $\Omega(1^2P_{1/2^-})$. (iv) The $\Omega(2250)$ resonance listed in RPP [2]

which is assigned as the $\Omega(1^4D_{5/2^+})$ state according to our previous studies [16]. The determined parameter set is listed in Table IV.

The predicted masses of the Ω baryons up to $N = 2$ shell have been given in Table I and also shown in Fig 1. For a comparison, some predictions from the other models are listed in Table I as well. It is found that the masses of the first radially excited states $\Omega(2^2S_{1/2^+})$ and $\Omega(2^4S_{3/2^+})$ obtained in present work are compatible with the predictions in Refs. [5, 12], however, the mass splitting between them $\Delta m \simeq 70$ MeV predicted in this work are obviously larger than the other model predictions. The mass of the $J^P = 1/2^+$ D -wave state $\Omega(1^4D_{1/2^+})$, 2141 MeV, predicted in this work is close to the predictions in Ref. [3, 12], however, our prediction is about 60-160 MeV lower than the those predicted in Refs. [5–8]. The masses of the $J^P = 3/2^+$ D -wave states $\Omega(1^4D_{3/2^+})$ and $\Omega(1^2D_{3/2^+})$ and their mass splitting $\Delta m \simeq 60$ MeV predicted in this work are close to those predicted in Refs. [7, 8]. The masses of the $J^P = 5/2^+$ D -wave states $\Omega(1^4D_{5/2^+})$ and $\Omega(1^2D_{5/2^+})$ and their mass splitting $\Delta m \simeq 50$ MeV predicted in this work are close to those predicted in Refs. [5, 7, 8]. The mass of the $J^P = 7/2^+$ D -wave state $\Omega(1^4D_{7/2^+})$ is close to those predictions in Refs. [5, 6], however, about 100 MeV higher than the predictions in Refs. [7, 8, 12]. Finally, it should be mentioned that if we consider a fairly large mass splitting $\Delta \simeq 50$ MeV between the two $1P$ -wave states $\Omega(1^2P_{3/2^-})$ and $\Omega(1^2P_{1/2^-})$ due to the spin-orbital interactions, the mass splitting between two adjacent D -wave spin-quartet states $\Omega(1^4D_J)$ and $\Omega(1^4D_{J+1})$ might reach up to $\sim 50 - 70$ MeV which is larger than the value $\sim 0 - 20$ MeV predicted in the literature [5–8, 12, 13].

TABLE III: The quantum numbers of Ω baryons up to $N = 2$ shell.

$n^{2S+1}L_{JP}$	c_i	s_{12}	s_3	S	l_ρ	l_λ	L	n_ρ	n_λ	N	J
$1^4S_{\frac{3}{2}^+}$	1	1	1/2	3/2	0	0	0	0	0	0	3/2
$1^2P_{\frac{1}{2}^-}$	$\sqrt{1/2}$	1	1/2	1/2	0	1	1	0	0	1	1/2
$1^2P_{\frac{3}{2}^-}$	$\sqrt{1/2}$	0	1/2	1/2	1	0	1	0	0	1	1/2
$1^2P_{\frac{3}{2}^-}$	$\sqrt{1/2}$	1	1/2	1/2	0	1	1	0	0	1	3/2
$1^2P_{\frac{3}{2}^-}$	$\sqrt{1/2}$	0	1/2	1/2	1	0	1	0	0	1	3/2
$2^2S_{\frac{1}{2}^+}$	$-\sqrt{1/4}$	1	1/2	1/2	0	0	0	1	0	2	1/2
$2^2S_{\frac{1}{2}^+}$	$\sqrt{1/4}$	1	1/2	1/2	0	0	0	0	1	2	1/2
$2^2S_{\frac{1}{2}^+}$	$\sqrt{1/2}$	0	1/2	1/2	1	1	0	0	0	2	1/2
$2^4S_{\frac{3}{2}^+}$	$\sqrt{1/2}$	1	1/2	3/2	0	0	0	1	0	2	3/2
$2^4S_{\frac{3}{2}^+}$	$\sqrt{1/2}$	1	1/2	3/2	0	0	0	0	1	2	3/2
$1^2D_{\frac{3}{2}^+}$	$\sqrt{1/4}$	1	1/2	1/2	2	0	2	0	0	2	3/2
$1^2D_{\frac{3}{2}^+}$	$-\sqrt{1/4}$	1	1/2	1/2	0	2	2	0	0	2	3/2
$1^2D_{\frac{3}{2}^+}$	$\sqrt{1/2}$	0	1/2	1/2	1	1	2	0	0	2	3/2
$1^2D_{\frac{3}{2}^+}$	$\sqrt{1/4}$	1	1/2	1/2	2	0	2	0	0	2	5/2
$1^2D_{\frac{3}{2}^+}$	$-\sqrt{1/4}$	1	1/2	1/2	0	2	2	0	0	2	5/2
$1^2D_{\frac{3}{2}^+}$	$\sqrt{1/2}$	0	1/2	1/2	1	1	2	0	0	2	5/2
$1^4D_{\frac{1}{2}^+}$	$\sqrt{1/2}$	1	1/2	3/2	2	0	2	0	0	2	1/2
$1^4D_{\frac{1}{2}^+}$	$\sqrt{1/2}$	1	1/2	3/2	0	2	2	0	0	2	1/2
$1^4D_{\frac{3}{2}^+}$	$\sqrt{1/2}$	1	1/2	3/2	2	0	2	0	0	2	3/2
$1^4D_{\frac{3}{2}^+}$	$\sqrt{1/2}$	1	1/2	3/2	0	2	2	0	0	2	3/2
$1^4D_{\frac{5}{2}^+}$	$\sqrt{1/2}$	1	1/2	3/2	2	0	2	0	0	2	5/2
$1^4D_{\frac{5}{2}^+}$	$\sqrt{1/2}$	1	1/2	3/2	0	2	2	0	0	2	5/2
$1^4D_{\frac{7}{2}^+}$	$\sqrt{1/2}$	1	1/2	3/2	2	0	2	0	0	2	7/2
$1^4D_{\frac{7}{2}^+}$	$\sqrt{1/2}$	1	1/2	3/2	0	2	2	0	0	2	7/2

TABLE IV: Quark model parameters used in this work.

m_s (GeV)	0.600
α_s	0.770
σ_{ss} (GeV)	0.600
b (GeV ²)	0.110
α_{SO} (GeV)	1.900
C_0 (GeV)	-0.694

III. STRONG AND RADIATIVE DECAYS

A. Framework

1. strong decay

In the chiral quark model, the effective low energy quark-pseudoscalar-meson coupling in the SU(3) flavor basis at tree level is given by [40]

$$H_m = \sum_j \frac{1}{f_m} \bar{\psi}_j \gamma_\mu \gamma_5 \psi_j \vec{\tau} \cdot \partial^\mu \vec{\phi}_m, \quad (28)$$

where f_m stands for the pseudoscalar meson decay constant. ψ_j corresponds to the j th quark field in a baryon and ϕ_m de-

notes the pseudoscalar meson octet

$$\phi_m = \begin{pmatrix} \frac{1}{\sqrt{2}}\pi^0 + \frac{1}{\sqrt{6}}\eta & \pi^+ & K^+ \\ \pi^- & -\frac{1}{\sqrt{2}}\pi^0 + \frac{1}{\sqrt{6}}\eta & K^0 \\ K^- & \bar{K}^0 & -\sqrt{\frac{2}{3}}\eta \end{pmatrix}. \quad (29)$$

To match the nonrelativistic baryon wave functions in the calculations, we adopt a nonrelativistic form of Eq.(28) for a baryon decay process [41–43], i.e.,

$$H_m^{nr} = \sum_j \left\{ \frac{\omega_m}{E_f + M_f} \sigma_j \cdot \mathbf{P}_f + \frac{\omega_m}{E_i + M_i} \sigma_j \cdot \mathbf{P}_i - \sigma_j \cdot \mathbf{q} + \frac{\omega_m}{2\mu_q} \sigma_j \cdot \mathbf{P}'_j \right\} I_j e^{-i\mathbf{q} \cdot \mathbf{r}_j}, \quad (30)$$

where (E_i, \mathbf{P}_i) , (E_f, \mathbf{P}_f) and (ω_m, \mathbf{q}) stand for the energy and three-vector momentum of the initial baryon, final baryon and meson, respectively; while M_i and M_f stand for the mass of the initial baryon and final baryon. We select the initial-baryon-rest system in the calculations. Then, $\mathbf{P}_i = 0$, $E_i = M_i$ and $\mathbf{P}_f = -\mathbf{q}$. In the Eq. (30) σ_j is the Pauli spin vector on the j th quark, and μ_q is a reduced mass expressed as $1/\mu_q = 1/m_j + 1/m'_j$. $\mathbf{P}'_j = \mathbf{P}_j - (m_j/M)\mathbf{P}_{c.m.}$ is the internal momentum of the j th quark in the baryon rest frame. The isospin operator I_j associated with the pseudoscalar meson is given by

$$I_j = \begin{cases} a_j^+(u)a_j(s) & \text{for } K^-, \\ a_j^+(d)a_j(s) & \text{for } \bar{K}^0, \\ \frac{1}{\sqrt{2}}[a_j^+(u)a_j(u) + a_j^+(d)a_j(d)] \cos \theta & \\ -a_j^+(s)a_j(s) \sin \theta & \text{for } \eta. \end{cases} \quad (31)$$

where $a_j^+(u, d, s)$ and $a_j(u, d, s)$ are the creation and annihilation operator for the u, d, s quarks on j th quark, while θ is the mixing angle of the η meson in the flavor basis. In this work we adopt $\theta = 41.2^\circ$ as that used in Ref. [44].

The decay amplitudes for a strong decay process $\mathcal{B} \rightarrow \mathcal{B}'\mathbb{M}$ can be calculated by

$$\mathcal{M}[\mathcal{B} \rightarrow \mathcal{B}'\mathbb{M}] = \langle \mathcal{B}' | H_m^{nr} | \mathcal{B} \rangle, \quad (32)$$

where $|\mathcal{B}'\rangle$ and $|\mathcal{B}\rangle$ stand for the wave functions of the final and initial baryon, respectively.

With the derived decay amplitudes, the partial decay width for the $\mathcal{B} \rightarrow \mathcal{B}'\mathbb{M}$ process is calculated by

$$\Gamma_m = \left(\frac{\delta}{f_m} \right)^2 \frac{(E_f + M_f)q}{4\pi M_i} \frac{1}{2J_i + 1} \sum_{J_{iz} J_{fz}} |\mathcal{M}_{J_{iz} J_{fz}}|^2, \quad (33)$$

where J_{iz} and J_{fz} represent the third components of the total angular momenta of the initial and final baryons, respectively. δ is a global parameter accounting for the strength of the quark-meson couplings.

The relativistic effects become significant when momentum \mathbf{q} of final baryon increases. As done in the literature [45–48], a commonly used Lorentz boost factor $\gamma_f \equiv M_f/E_f$ is introduced into the decay amplitudes

$$\mathcal{M}(\mathbf{q}) \rightarrow \gamma_f \mathcal{M}(\gamma_f \mathbf{q}), \quad (34)$$

to partly remedy the inadequacy of the nonrelativistic wave function as the momentum \mathbf{q} increases. In most decays, the sum of the masses of the final hadron states is not far away from the mass of the initial state, the three momenta \mathbf{q} carried by the final states are relatively small, which means the non-relativistic prescription is reasonable and corrections from the Lorentz boost are not drastic.

2. radiative decay

The quark-photon EM coupling at the tree level is adopted as

$$H_e = - \sum_j e_j \bar{\psi}_j \gamma_\mu^j A^\mu(\mathbf{k}, \mathbf{r}_j) \psi_j. \quad (35)$$

The photon field A^μ has three momentum \mathbf{k} , and the constituent quark ψ_j carries a charge e_j . While \mathbf{r}_j stands for the coordinate of the j th quark.

In order to match the nonrelativistic wave functions of the baryons, we should adopt the nonrelativistic form of Eq. (35) in the calculations. Including the effects of the binding potential between quarks [49], for emitting a photon the nonrelativistic expansion of H_e may be written as [42, 43, 50]

$$h_e \simeq \sum_j \left[e_j \mathbf{r}_j \cdot \boldsymbol{\epsilon} - \frac{e_j}{2m_j} \boldsymbol{\sigma}_j \cdot (\boldsymbol{\epsilon} \times \hat{\mathbf{k}}) \right] e^{-i\mathbf{k} \cdot \mathbf{r}_j}, \quad (36)$$

where m_j and $\boldsymbol{\sigma}_j$ stand for the constituent mass and Pauli spin vector for the j th quark. The vector $\boldsymbol{\epsilon}$ is the polarization vector of the photon. This nonrelativistic EM transition operator has been widely applied to meson photoproduction reactions [41–45, 51–57].

Then, the standard helicity transition amplitude \mathcal{A}_λ between the initial baryon state $|\mathcal{B}\rangle$ and the final baryon state $|\mathcal{B}'\rangle$ can be calculated by

$$\mathcal{A}_\lambda = -i \sqrt{\frac{\omega_\gamma}{2}} \langle \mathcal{B}' | h_e | \mathcal{B} \rangle. \quad (37)$$

where ω_γ is the photon energy.

Finally, one can calculate the EM decay width by

$$\Gamma_\gamma = \frac{|\mathbf{k}|^2}{\pi} \frac{2}{2J_i + 1} \frac{M_f}{M_i} \sum_{J_{fz}, J_{iz}} |\mathcal{A}_{J_{fz}, J_{iz}}|^2, \quad (38)$$

where J_i is the total angular momentum of an initial meson, J_{fz} and J_{iz} are the components of the total angular momenta along the z axis of initial and final mesons, respectively.

TABLE V: The masses (MeV) of the final mesons and baryons.

	Ξ^0	Ξ^-	$\Xi(1530)^0$	$\Xi(1530)^-$	K^-	\bar{K}^0	η
Mass	1315	1322	1532	1535	494	498	548

B. Parameters

In the calculation, the constituent quark masses for the u , d , and s quarks are taken with $m_u = m_d = 350$ MeV and $m_s = 600$ MeV. The masses of the Ω baryon states are adopted the determinations by solving the Schrödinger equation in Sec.II. It should be mentioned that, we do not directly adopt the numerical wave functions of Ω baryons calculated by solving the Schrödinger equation. For simplicity, we first fit them with a single Gaussian (SG) form by reproducing the root-mean-square radius of the ρ -mode excitations. The determined harmonic oscillator strength parameters, α , for corresponding Ω baryons are listed in Table VI. It is found determined parameters α are very close to the value ~ 400 MeV often adopted for the SHO wave functions in the literature.

Furthermore, in the calculations of the strong decays, for simplicity, the wave functions of Ξ and $\Xi(1530)$ baryons appearing in the final states are adopted the SHO form as adopted in Ref. [37]. The harmonic oscillator strength parameter α_ρ for the ρ -oscillator in the spatial wave function is taken as $\alpha_\rho = 400$ MeV, while the parameter α_λ for the λ -oscillator is related to α_ρ with $\alpha_\lambda = \sqrt[3]{3m_u/(2m_s + m_u)}\alpha_\rho$ [37]. The masses of the mesons and baryons in the final states are taken from the RPP [2] and have been collected in Table V. The decay constants for K and η mesons are taken as $f_K = f_\eta = 160$ MeV. For the global parameter δ , we fix its value the same as the previous study of the strong decays of Ξ and Ω baryons [16, 37], i.e., $\delta = 0.576$. The strong and radiative decay widths of Ω baryons up to $N = 2$ shell are listed in Table VI and Table VII, respectively.

IV. DISCUSSIONS

A. 1P states

There are two 1P-wave states $\Omega(1^2P_{1/2^-})$ and $\Omega(1^2P_{3/2^-})$ according to the quark model classification. By analyzing the strong decay properties with SHO wave functions, it is found that the newly observed $\Omega(2012)$ resonance can be assigned to the $J^P = 3/2^-$ state $\Omega(1^2P_{3/2^-})$ in Refs. [16, 17].

1. $\Omega(2012)$

In this work, by using the wave function calculated from the potential model, we reanalyze the strong decays of the $\Omega(2012)$ state within the chiral quark model. As a candidate of the $J^P = 3/2^-$ state $\Omega(1^2P_{3/2^-})$ ($(170, 2^+ 10, 1, 1, 3/2^-)$), both the predicted width

$$\Gamma_{\text{total}}^{\text{th}}[\Omega(2012)] = 5.69 \text{ MeV}, \quad (39)$$

and branching fraction ratio

$$\mathcal{R} = \frac{\Gamma[\Omega(2012) \rightarrow \Xi^0 K^-]}{\Gamma[\Omega(2012) \rightarrow \Xi^- \bar{K}^0]} \simeq 1.1, \quad (40)$$

TABLE VI: The strong decay widths (MeV) of Ω baryons up to $N = 2$ shell. Γ_{total}^{th} stands for the total decay width and \mathcal{B} represents the ratio of the branching fraction $\Gamma[\Xi K]/\Gamma[\Xi(1530)K]$.

$n^{2S+1}L_{JP}$	Mass	$\alpha(\text{MeV})$	$\Gamma[\Xi K]$		$\Gamma[\Xi(1530)K]$		$\Gamma[\Omega(1672)\eta]$		Γ_{total}^{th}		\mathcal{B}	
			Ours	Ref. [16]	Ours	Ref. [16]	Ours	Ref. [16]	Ours	Ref. [16]	Ours	Ref. [16]
$1^2P_{\frac{1}{2}^-}$	1957	428	12.43	12.64	12.43	12.64
$1^2P_{\frac{3}{2}^-}$	2012	411	5.69	5.81	5.69	5.81
$2^2S_{\frac{1}{2}^+}$	2232	387	0.04	0.27	5.09	8.32	0.006	0.08	5.14	8.67	0.008	0.03
$2^4S_{\frac{3}{2}^+}$	2159	381	0.99	4.72	5.12	8.96	6.11	13.68	0.19	0.53
$1^2D_{\frac{3}{2}^+}$	2245	394	2.49	2.52	4.27	4.24	0.055	0.06	6.82	6.82	0.58	0.59
$1^2D_{\frac{5}{2}^+}$	2303	380	3.07	3.04	14.30	14.51	1.65	1.81	19.02	19.36	0.21	0.21
$1^4D_{\frac{1}{2}^+}$	2141	413	39.52	39.34	2.17	2.21	41.69	41.55	18.21	17.80
$1^4D_{\frac{3}{2}^+}$	2188	399	20.25	20.26	10.93	10.92	31.18	31.18	1.85	1.86
$1^4D_{\frac{5}{2}^+}$	2252	383	5.28	5.21	21.37	21.48	0.79	0.90	27.44	27.59	0.25	0.24
$1^4D_{\frac{7}{2}^+}$	2321	367	34.38	34.36	7.17	7.00	0.066	0.13	41.62	41.49	4.79	4.91

TABLE VII: Partial widths (KeV) of radiative decays for the Ω baryons up to $N = 2$ shell.

Initial state	$\Gamma[\Omega(1672)\gamma]$	
$\Omega(1^2P_{1/2^-})$	4.68	
$\Omega(2012)$	9.52	
Initial state	$\Gamma[\Omega(1^2P_{1/2^-})\gamma]$	$\Gamma[\Omega(2012)\gamma]$
$\Omega(2^2S_{1/2^+})$	10.16	15.71
$\Omega(2^4S_{3/2^+})$	0.01	0.06
$\Omega(1^2D_{3/2^+})$	46.13	11.53
$\Omega(1^2D_{5/2^+})$	1.13	60.78
$\Omega(1^4D_{1/2^+})$	0.0002	0.02
$\Omega(1^4D_{3/2^+})$	0.99	0.02
$\Omega(1^4D_{5/2^+})$	0.99	1.10
$\Omega(1^4D_{7/2^+})$	0.01	3.99

are in good agreement with the measured width $\Gamma^{\text{exp}} = 6.4^{+2.5}_{-2.0} \pm 0.6$ MeV and ratio $\mathcal{R}^{\text{exp}} = 1.2 \pm 0.3$ of the newly observed $\Omega(2012)$ state, and also are consistent with the predictions with the SHO wave functions [16]. Furthermore, we study the radiative decay properties of $\Omega(2012)$. The partial radiative decay width for the $\Omega(2012) \rightarrow \Omega(1672)\gamma$ process is predicted to be

$$\Gamma[\Omega(2012) \rightarrow \Omega(1672)\gamma] = 9.52 \text{ keV}. \quad (41)$$

Combining this partial width with the measured total width of $\Omega(2012)$, we estimate the branching fraction for this radiative decay process:

$$Br[\Omega(2012) \rightarrow \Omega(1672)\gamma] \simeq 1.67 \times 10^{-3}. \quad (42)$$

The radiative process $\Omega(2012) \rightarrow \Omega(1672)\gamma$ may be observed in forthcoming experiments at Belle II. It should be mentioned that the $\Gamma[\Omega(2012) \rightarrow \Omega(1672)\gamma] = 9.52$ keV predicted in this work is about a factor 2 smaller than the early prediction within a nonrelativistic potential model in Ref. [58].

2. $\Omega(1^2P_{1/2^-})$

The $J^P = 1/2^-$ state $\Omega(1^2P_{1/2^-})$ ($(70,^2 10, 1, 1, 1/2^-)$) might have mass of ~ 1950 MeV, which is about 50 MeV lower than that of the $J^P = 3/2^-$ state $\Omega(1^2P_{3/2^-})$ according to the predictions within the Lattice QCD [13] and the relativized quark models [5, 6]. The measured ΞK invariant mass distributions from Belle show that there is a weak enhancement around 1950 MeV [15], which may be a weak hint of $J^P = 1/2^-$ state $\Omega(1^2P_{1/2^-})$. Thus, in this work, we adjust the potential parameters to determine the mass of $\Omega(1^2P_{1/2^-})$ with ~ 1957 MeV. By using this mass and the wave function calculated from the potential model, we predict the total width of $\Omega(1^2P_{1/2^-})$ to be

$$\Gamma_{total}^{th}[\Omega(1^2P_{1/2^-})] \simeq 12 \text{ MeV}, \quad (43)$$

which is compatible with the previous result with the SHO wave function in the chiral quark model [16], while about factor of 4 narrower than that of the 3P_0 model [17]. The total width of $\Omega(1^2P_{1/2^-})$ should be saturated by the $\Xi^0 K^-$ and $\Xi^- \bar{K}^0$ channels. The branching fraction ratio between $\Xi^0 K^-$ and $\Xi^- \bar{K}^0$ is predicted to be

$$\mathcal{R} = \frac{\Gamma[\Omega(1^2P_{1/2^-}) \rightarrow \Xi^0 K^-]}{\Gamma[\Omega(1^2P_{1/2^-}) \rightarrow \Xi^- \bar{K}^0]} \simeq 0.97. \quad (44)$$

The narrow width and the only dominant ΞK decay mode of the $J^P = 1/2^-$ state $\Omega(1^2P_{1/2^-})$ indicate that it has a large potential to be established as future experimental statistics increases.

We further study the radiative decays of the $J^P = 1/2^-$ state $\Omega(1^2P_{1/2^-})$. The partial decay width of the $\Omega(1672)\gamma$ channel is predicted to be

$$\Gamma[\Omega(1^2P_{1/2^-}) \rightarrow \Omega(1672)\gamma] \simeq 4.68 \text{ keV}, \quad (45)$$

which is about a factor 3 smaller than the early prediction within a nonrelativistic potential model in Ref. [58]. Combining our predictions of the radiative decay and total decay width of $\Omega(1^2P_{1/2^-})$, we obtain a branching fraction

$$Br[\Omega(1^2P_{1/2^-}) \rightarrow \Omega(1672)\gamma] \simeq 3.8 \times 10^{-4}, \quad (46)$$

which is about an order smaller than $Br[\Omega(2012) \rightarrow \Omega(1672)\gamma]$. Thus, the radiative decay of the $J^P = 1/2^-$ Ω state into $\Omega(1672)\gamma$ may be more difficultly observed than $\Omega(2012)$.

B. 1D states

There are six 1D-wave states $\Omega(1^2D_{3/2^+,5/2^+})$ and $\Omega(1^4D_{1/2^+,3/2^+,5/2^+,7/2^+})$ in the constituent quark model. According to our quark model predictions (see Table I), it is found that in these 1D-wave states the $\Omega(1^4D_{1/2^+})$ has the lowest mass of ~ 2141 MeV, the next low mass 1D-wave state is $\Omega(1^4D_{3/2^+})$, whose mass is 2188 MeV. The mass splitting between these two states, ~ 50 MeV, predicted in this work is obviously larger than $\sim 0 - 20$ MeV predicted in Refs. [5–8, 12, 13]. The 1D-wave states $\Omega(1^4D_{5/2^+})$ and $\Omega(1^2D_{3/2^+})$ have a similar mass in the range of $\sim 2250 \pm 10$ MeV; while $\Omega(1^4D_{7/2^+})$ and $\Omega(1^2D_{5/2^+})$ have a similar mass around ~ 2300 MeV. Based on the obtained decay properties and mass spectrum, some discussions about these 1D-wave states are given as follows.

1. $\Omega(1^4D_{1/2^+})$

As the lowest 1D-wave state, the $\Omega(1^4D_{1/2^+})$ ($[56,^4 10, 2, 2, 1/2^+]$) state may have a mass of ~ 2141 MeV. Its decay width is predicted to be

$$\Gamma_{\text{total}}^{\text{th}}[\Omega(1^4D_{1/2^+})] \simeq 42 \text{ MeV}, \quad (47)$$

which is consistent with the prediction with the SHO wave function [16]. This state dominantly decays into the ΞK channel, the decay rates into the $\Xi(1530)K$ channel is tiny. The branching fraction ratio between ΞK and $\Xi(1530)K$ channels is predicted to be

$$\frac{\Gamma[\Omega(1^4D_{1/2^+}) \rightarrow \Xi(1530)K]}{\Gamma[\Omega(1^4D_{1/2^+}) \rightarrow \Xi K]} \simeq 5\%. \quad (48)$$

This $J^P = 1/2^+$ 1D-wave state might be found in the ΞK invariant mass spectrum around 2.14 GeV.

2. $\Omega(1^4D_{3/2^+})$

For the next low mass 1D-wave state $\Omega(1^4D_{3/2^+})$ ($[56,^4 10, 2, 2, 3/2^+]$), its mass ~ 2188 MeV is about 50 MeV higher than that of $\Omega(1^4D_{1/2^+})$. The $\Omega(1^4D_{3/2^+})$ state mainly decays into ΞK and $\Xi(1530)K$ channels with a moderate total width

$$\Gamma_{\text{total}}^{\text{th}}[\Omega(1^4D_{3/2^+})] \simeq 31 \text{ MeV}. \quad (49)$$

The branching fraction ratio between ΞK and $\Xi(1530)K$ channels is predicted to be

$$\frac{\Gamma[\Omega(1^4D_{3/2^+}) \rightarrow \Xi(1530)K]}{\Gamma[\Omega(1^4D_{3/2^+}) \rightarrow \Xi K]} \simeq 0.54. \quad (50)$$

The above predictions are consistent with the previous predictions with the SHO wave function [16]. To search for the missing $\Omega(1^4D_{3/2^+})$, both ΞK and $\Xi(1530)K$ channels are worth observing.

3. $\Omega(1^2D_{3/2^+})$

The mass of the $J^P = 3/2^+$ state $\Omega(1^2D_{3/2^+})$ ($[70,^2 10, 2, 2, 3/2^+]$) is predicted to be ~ 2245 MeV in this work, which is compatible with the predictions in Refs. [7, 8]. The $\Omega(1^2D_{3/2^+})$ state might be a narrow state with a width of

$$\Gamma_{\text{total}}^{\text{th}}[\Omega(1^2D_{3/2^+})] \simeq 7 \text{ MeV}. \quad (51)$$

The $\Omega(1^2D_{3/2^+})$ state dominantly decays into $\Xi(1530)K$ and ΞK channels. The partial width ratio between these two decay channels is predicted to be

$$\frac{\Gamma[\Omega(1^2D_{3/2^+}) \rightarrow \Xi(1530)K]}{\Gamma[\Omega(1^2D_{3/2^+}) \rightarrow \Xi K]} \simeq 1.7. \quad (52)$$

To establish the $\Omega(1^2D_{3/2^+})$ state, both the $\Xi(1530)K$ and ΞK final states are worth observing in future experiments.

Furthermore, it is interesting to find that the radiative decay rates of $\Omega(1^2D_{3/2^+})$ into $\Omega(1^2P_{1/2^-})\gamma$ and $\Omega(2012)\gamma$ are relatively large. The radiative partial widths are predicted to be

$$\Gamma[\Omega(1^2D_{3/2^+}) \rightarrow \Omega(1^2P_{1/2^-})\gamma] \simeq 46 \text{ keV}, \quad (53)$$

$$\Gamma[\Omega(1^2D_{3/2^+}) \rightarrow \Omega(2012)\gamma] \simeq 12 \text{ keV}. \quad (54)$$

Combining them with predicted total width of $\Omega(1^2D_{3/2^+})$, we obtain the branching fractions

$$Br[\Omega(1^2D_{3/2^+}) \rightarrow \Omega(1^2P_{1/2^-})\gamma] \simeq 6.8 \times 10^{-3}, \quad (55)$$

$$Br[\Omega(1^2D_{3/2^+}) \rightarrow \Omega(2012)\gamma] \simeq 1.7 \times 10^{-3}. \quad (56)$$

The radiative transitions $\Omega(1^2D_{3/2^+}) \rightarrow \Omega(1^2P_{1/2^-})\gamma$ and $\Omega(1^2D_{3/2^+}) \rightarrow \Omega(2012)\gamma$ might be observed in future experiments.

4. $\Omega(1^4D_{5/2^+})$

The $J^P = 5/2^+$ state $\Omega(1^4D_{5/2^+})$ ($[56,^4 10, 2, 2, 5/2^+]$) has a mass of ~ 2252 MeV. The previous study [16] suggested that the $\Omega(1^4D_{5/2^+})$ state might be a good candidate of $\Omega(2250)$ listed in RPP [2]. Assigning $\Omega(2250)$ as $\Omega(1^4D_{5/2^+})$, with the wave function calculated from the potential model, its total width is predicted to be

$$\Gamma_{\text{total}}^{\text{th}}[\Omega(2250)] \simeq 27 \text{ MeV}, \quad (57)$$

which is close to the lower limit of the measured width $\Gamma = 55 \pm 18$ MeV. The strong decays of $\Omega(2250)$ are dominated by the $\Xi(1530)K$ mode, while the decay rate into the ΞK is

sizeable. The partial width ratio between $\Xi(1530)K$ and ΞK is predicted to be

$$\mathcal{R} = \frac{\Gamma[\Omega(2250) \rightarrow \Xi(1530)K]}{\Gamma[\Omega(2250) \rightarrow \Xi K]} \simeq 4.0. \quad (58)$$

The decay mode is consistent with the observations that the $\Omega(2250)$ was seen in the $\Xi(1530)K$ and $\Xi^-\pi^+K^-$ channels. Thus, the $\Omega(2250)$ favors the assignment of $\Omega(1^4D_{5/2^+})$. This conclusion is in agreement with that obtained with a SHO wave function in Ref. [16].

It should be mentioned that the $J^P = 5/2^+$ state $\Omega(1^4D_{5/2^+})$ may highly overlap with the $J^P = 3/2^+$ state $\Omega(1^2D_{3/2^+})$, and the mass splitting between them is only several MeV in present calculations. Thus, it may bring some difficulties to distinguish them in experiments.

5. $\Omega(1^2D_{5/2^+})$

The $J^P = 5/2^+$ state $\Omega(1^2D_{5/2^+})$ ($[70,^2 10, 2, 2, 5/2^+]$) has a mass of ~ 2.3 GeV according to our predictions, which is close to the predictions in Refs. [5, 7, 8]. Its total width is predicted to be

$$\Gamma_{\text{total}}^{\text{th}}[\Omega(1^2D_{5/2^+})] \simeq 19 \text{ MeV}. \quad (59)$$

The $\Omega(1^2D_{5/2^+})$ state dominantly decays into $\Xi(1530)K$ channel, the decay rate into the ΞK channel is relatively small. The partial width ratio between these two channels is predicted to be

$$\frac{\Gamma[\Omega(1^2D_{5/2^+}) \rightarrow \Xi K]}{\Gamma[\Omega(1^2D_{5/2^+}) \rightarrow \Xi(1530)K]} \simeq 0.21. \quad (60)$$

The strong decay properties predicted in this work is close to the previous results obtained with a simple harmonic oscillator wave function in Ref. [16].

Furthermore, it is interesting to find that the radiative decay rate of $\Omega(1^2D_{5/2^+})$ into $\Omega(2012)\gamma$ is large. Its radiative partial width is predicted to be

$$\Gamma[\Omega(1^2D_{5/2^+}) \rightarrow \Omega(2012)\gamma] \simeq 61 \text{ keV}. \quad (61)$$

Combining it with the predicted total width of $\Omega(1^2D_{5/2^+})$, we find that the branching fraction can reach up to

$$Br[\Omega(1^2D_{5/2^+}) \rightarrow \Omega(2012)\gamma] \simeq 3.2 \times 10^{-3}. \quad (62)$$

The radiative decay process $\Omega(1^2D_{5/2^+}) \rightarrow \Omega(2012)\gamma$ might be useful for searching for the missing $\Omega(1^2D_{5/2^+})$ state.

6. $\Omega(1^4D_{7/2^+})$

In this work, the $J^P = 7/2^+$ state $\Omega(1^4D_{7/2^+})$ ($[56,^4 10, 2, 2, 7/2^+]$) is predicted to be the highest $1D$ -wave state. Its mass is estimated to be ~ 2321 MeV, which is close to the predictions in Refs. [5, 6]. The total width of $\Omega(1^4D_{7/2^+})$ is predicted to be

$$\Gamma_{\text{total}}^{\text{th}}[\Omega(1^4D_{7/2^+})] \simeq 42 \text{ MeV}. \quad (63)$$

This state dominantly decays into ΞK channel, the decay rate into the $\Xi(1530)K$ channel is relatively small. The partial width ratio between these two channels is predicted to be

$$\frac{\Gamma[\Omega(1^4D_{7/2^+}) \rightarrow \Xi(1530)K]}{\Gamma[\Omega(1^4D_{7/2^+}) \rightarrow \Xi K]} \simeq 0.21. \quad (64)$$

It should be mentioned that the mass of $\Omega(1^4D_{7/2^+})$ is similar to that of $\Omega(1^2D_{5/2^+})$, the mass splitting between these two states is only ~ 18 MeV according to our predictions. By observing the $\Xi(1530)K$ and ΞK invariant mass distributions, one may find two largely overlapping states around 2.3 GeV. The $\Omega(1^4D_{7/2^+})$ state mainly decays into ΞK channel, while $\Omega(1^2D_{5/2^+})$ dominantly decays into $\Xi(1530)K$ channel.

C. $2S$ states

There are two $2S$ -wave states $\Omega(2^2S_{1/2^+})$ and $\Omega(2^4S_{3/2^+})$ according to the quark model classification. The mass splitting between these two radial excitations are about 70 MeV. With the spectrum of the $2S$ states calculated in this work, we further analyze their strong and radiative decay properties, the results have been collected Tables VI and VII.

1. $\Omega(2^2S_{1/2^+})$

The $J^P = 1/2^+$ state $\Omega(2^2S_{1/2^+})$ ($[70,^2 10, 2, 0, 1/2^+]$) has a mass of ~ 2232 MeV according to our predictions, which is close to the predictions in Refs. [5, 7, 8, 12]. The $\Omega(2^2S_{1/2^+})$ state might be narrow state with a width of

$$\Gamma_{\text{total}}^{\text{th}}[\Omega(2^2S_{1/2^+})] \simeq 5 \text{ MeV}. \quad (65)$$

The $\Omega(2^2S_{1/2^+})$ state dominantly decays into the $\Xi(1530)K$ channel. The branching fraction ratio between ΞK and $\Xi(1530)K$ channels is predicted to be

$$\frac{\Gamma[\Omega(2^2S_{1/2^+}) \rightarrow \Xi K]}{\Gamma[\Omega(2^2S_{1/2^+}) \rightarrow \Xi(1530)K]} \simeq 1\%. \quad (66)$$

Furthermore, it is interesting to find that the radiative decay rates of $\Omega(2^2S_{1/2^+})$ into $\Omega(1^2P_{1/2^-})\gamma$ and $\Omega(2012)\gamma$ final states are relatively large. The radiative partial widths are predicted to be

$$\Gamma[\Omega(2^2S_{1/2^+}) \rightarrow \Omega(1^2P_{1/2^-})\gamma] \simeq 10 \text{ keV}, \quad (67)$$

$$\Gamma[\Omega(2^2S_{1/2^+}) \rightarrow \Omega(2012)\gamma] \simeq 16 \text{ keV}. \quad (68)$$

Combining it with predicted total width of $\Omega(2^2S_{1/2^+})$, we obtain the branching fraction

$$Br[\Omega(2^2S_{1/2^+}) \rightarrow \Omega(1^2P_{1/2^-})\gamma] \simeq 1.8 \times 10^{-3}, \quad (69)$$

$$Br[\Omega(2^2S_{1/2^+}) \rightarrow \Omega(2012)\gamma] \simeq 2.8 \times 10^{-3}. \quad (70)$$

The radiative processes $\Omega(2^2S_{1/2^+}) \rightarrow \Omega(1^2P_{1/2^-})\gamma$ and $\Omega(2^2S_{1/2^+}) \rightarrow \Omega(2012)\gamma$ might be observed in future experiments.

2. $\Omega(2^4S_{3/2^+})$

The $J^P = 3/2^+$ state $\Omega(2^4S_{3/2^+})$ ($[56,^4 10, 2, 0, 3/2^+]$) has a mass of ~ 2159 MeV according to our predictions, which is close to the predictions in Refs. [5, 6, 12]. The $\Omega(2^4S_{3/2^+})$ state width is predicted to be

$$\Gamma_{\text{total}}^{\text{th}}[\Omega(2^4S_{3/2^+})] \simeq 6 \text{ MeV}. \quad (71)$$

The $\Omega(2^4S_{3/2^+})$ state dominantly decays into the $\Xi(1530)K$ channel. The branching fraction ratio between ΞK and $\Xi(1530)K$ channels is predicted to be

$$\frac{\Gamma[\Omega(2^4S_{3/2^+}) \rightarrow \Xi(1530)K]}{\Gamma[\Omega(2^4S_{3/2^+}) \rightarrow \Xi K]} \simeq 5.2. \quad (72)$$

To establish the $\Omega(2^4S_{3/2^+})$ state, the $\Xi(1530)K$ invariant mass spectrum around 2.1 – 2.2 GeV is worth observing in future experiments.

Finally, it should be mentioned that the strong decay of the $2S$ -wave states are sensitive to the details of the wave functions. The strong decay properties in present work with the wave functions calculated from the potential model show some obvious differences from the results with the SHO wave functions [16].

V. SUMMARY

In this work, combining the recent developments of the observations of Ω states in experiments we calculate the Ω spectrum up to the $N = 2$ shell within a nonrelativistic constituent quark potential model. Furthermore, the strong and radiative decay properties for the Ω resonances within the $N = 2$ shell are estimated by using the predicted masses and wave functions from the potential model.

The $\Omega(2012)$ resonance is most likely to be the spin-parity $J^P = 3/2^-$ $1P$ -wave state $\Omega(1^2P_{3/2^-})$. Both the mass and decay properties predicted in theory are consistent with the observations. The $\Omega(2012)$ resonance may be observed in the radiative decay channel $\Omega(1672)\gamma$, the branching fraction is predicted to be $O(10^{-3})$. The other $1P$ -wave state with $J^P = 1/2^-$ is also a narrow state with a width of ~ 12 MeV, which is about a factor 2 – 3 broader than that of $\Omega(2012)$. If more data were accumulated, the $J^P = 1/2^-$ state may be clearly established in the $\Xi^- \bar{K}^0$ and $\Xi^0 K^-$ invariant mass distributions around 1.95 GeV.

The $\Omega(2250)$ resonance may be a good candidate for the $J^P = 5/2^+$ $1D$ -wave state $\Omega(1^4D_{5/2^+})$, with this assignment

both the mass and strong decay properties of $\Omega(2250)$ can be reasonably understood in the quark model. It should be mentioned that the $J^P = 5/2^+$ $1D$ -wave state $\Omega(1^4D_{5/2^+})$ may highly overlap with the $J^P = 3/2^+$ $1D$ -wave state $\Omega(1^2D_{3/2^+})$. This state might be a narrow state with a width of several MeV and mainly decays into ΞK and $\Xi(1530)K$ channels. The measurements of the partial width ratio between these two channels might be helpful to distinguish the $\Omega(1^2D_{3/2^+})$ state from the $\Omega(1^4D_{5/2^+})$ state in experiments. Furthermore, the $\Omega(1^2D_{3/2^+})$ state might be established in the radiative decay channel $\Omega(2012)\gamma$, the predicted branching fraction can reach up to $O(10^{-3})$.

For the other $1D$ -wave states, it is found that both $\Omega(1^4D_{7/2^+})$ and $\Omega(1^4D_{1/2^+})$ dominantly decay into the ΞK channel with a width of ~ 40 MeV, they may be established in the ΞK invariant mass spectrum around 2.3 GeV and 2.1 GeV, respectively. The $\Omega(1^2D_{5/2^+})$ state dominantly decay into the $\Xi(1530)K$ channel with a narrow width of 19 MeV, it is worth to looking for in the $\Xi(1530)K$ invariant mass spectrum around 2.3 GeV. The $\Omega(1^4D_{3/2^+})$ state has a width of ~ 30 MeV, it mainly decays into both ΞK and $\Xi(1530)K$ channels. To look for this missing state, both ΞK and $\Xi(1530)K$ invariant mass distributions around 2.2 GeV are worth observing in future experiments.

For the $2S$ -wave states $\Omega(2^2S_{1/2^+})$ and $\Omega(2^4S_{3/2^+})$ might be very narrow state with a width of several MeV. The mass splitting between these two states is about 70 MeV. They may be established in the $\Xi(1530)K$ invariant mass spectrum around 2.2 GeV. It should be mentioned that the strong decays of the $2S$ -wave states show some sensitivities to the details of the wave functions, the strong decay properties of these $2S$ -wave states predicted in this work have some differences from those calculated with the SHO wave functions. The $\Omega(2^2S_{1/2^+})$ state might have relatively large radiative decay rates into the $1P$ -wave Ω states with a branching fraction $O(10^{-3})$. The $\Omega(2^2S_{1/2^+})$ state might be established with the $\Omega(2012)\gamma$ final state.

Acknowledgement

The authors thank Dr. Li-Ye Xiao for providing the strong decay results of SHO. MS also thanks Prof. Fei Huang for very helpful discussions of the baryon spectrum. This work is supported by the National Natural Science Foundation of China under Grants No. 11775078, No. U1832173, and No. 11705056.

-
- [1] V. E. Barnes *et al.*, Observation of a Hyperon with Strangeness -3, Phys. Rev. Lett. **12**, 204 (1964).
 [2] M. Tanabashi *et al.* [Particle Data Group], Review of Particle Physics, Phys. Rev. D **98**, 030001 (2018).
 [3] Y. Oh, Xi and Omega baryons in the Skyrme model, Phys. Rev. D **75**, 074002 (2007).

- [4] U. Loring, B. C. Metsch and H. R. Petry, The Light baryon spectrum in a relativistic quark model with instanton induced quark forces: The Nonstrange baryon spectrum and ground states, Eur. Phys. J. A **10**, 395 (2001).
 [5] S. Capstick and N. Isgur, Baryons in a Relativized Quark Model with Chromodynamics, Phys. Rev. D **34**, 2809 (1986).

- [6] R. N. Faustov and V. O. Galkin, Strange baryon spectroscopy in the relativistic quark model, *Phys. Rev. D* **92**, 054005 (2015).
- [7] K. T. Chao, N. Isgur and G. Karl, Strangeness -2 and -3 Baryons in a Quark Model With Chromodynamics, *Phys. Rev. D* **23**, 155 (1981).
- [8] Y. Chen and B. Q. Ma, Light flavor baryon spectrum with higher order hyperfine interactions, *Nucl. Phys. A* **831**, 1 (2009).
- [9] C. S. An, B. C. Metsch and B. S. Zou, Mixing of the low-lying three- and five-quark Ω states with negative parity, *Phys. Rev. C* **87**, 065207 (2013).
- [10] C. S. An and B. S. Zou, Low-lying Ω states with negative parity in an extended quark model with Nambu-Jona-Lasinio interaction, *Phys. Rev. C* **89**, 055209 (2014).
- [11] C. Hayne and N. Isgur, Beyond the Wave Function at the Origin: Some Momentum Dependent Effects in the Nonrelativistic Quark Model, *Phys. Rev. D* **25**, 1944 (1982).
- [12] M. Pervin and W. Roberts, Strangeness -2 and -3 baryons in a constituent quark model, *Phys. Rev. C* **77**, 025202 (2008).
- [13] G. P. Engel *et al.* [BGR Collaboration], QCD with Two Light Dynamical Chirally Improved Quarks: Baryons, *Phys. Rev. D* **87**, 074504 (2013).
- [14] J. Liang *et al.* [CLQCD Collaboration], Spectrum and Bethe-Salpeter amplitudes of Ω baryons from lattice QCD, *Chin. Phys. C* **40**, 041001 (2016).
- [15] J. Yelton *et al.* [Belle Collaboration], Observation of an Excited Ω^- Baryon, *Phys. Rev. Lett.* **121**, no. 5, 052003 (2018).
- [16] L. Y. Xiao and X. H. Zhong, Possible interpretation of the newly observed $\Omega(2012)$ state, *Phys. Rev. D* **98**, 034004 (2018).
- [17] Z. Y. Wang, L. C. Gui, Q. F. L., L. Y. Xiao and X. H. Zhong, Newly observed $\Omega(2012)$ state and strong decays of the low-lying Ω excitations, *Phys. Rev. D* **98**, 114023 (2018).
- [18] T. M. Aliev, K. Azizi, Y. Sarac and H. Sundu, Interpretation of the newly discovered $\Omega(2012)$, *Phys. Rev. D* **98**, 014031 (2018).
- [19] T. M. Aliev, K. Azizi, Y. Sarac and H. Sundu, Nature of the $\Omega(2012)$ through its strong decays, *Eur. Phys. J. C* **78**, 894 (2018).
- [20] M. V. Polyakov, H. D. Son, B. D. Sun and A. Tandogan, $\Omega(2012)$ through the looking glass of flavour SU(3), *Phys. Lett. B* **792**, 315 (2019).
- [21] M. P. Valderrama, $\Omega(2012)$ as a hadronic molecule, *Phys. Rev. D* **98**, 054009 (2018).
- [22] R. Pavao and E. Oset, Coupled channels dynamics in the generation of the $\Omega(2012)$ resonance, *Eur. Phys. J. C* **78**, 857 (2018).
- [23] Y. H. Lin and B. S. Zou, Hadronic molecular assignment for the newly observed Ω^* state, *Phys. Rev. D* **98**, 056013 (2018).
- [24] Y. Huang, M. Z. Liu, J. X. Lu, J. J. Xie and L. S. Geng, Strong decay modes $\bar{K}\Xi$ and $\bar{K}\Xi\pi$ of the $\Omega(2012)$ in the $\bar{K}\Xi(1530)$ and $\eta\Omega$ molecular scenario, *Phys. Rev. D* **98**, 076012 (2018).
- [25] S. Jia *et al.* [Belle Collaboration], Search for $\Omega(2012) \rightarrow K\Xi(1530) \rightarrow K\pi\Xi$ at Belle, *Phys. Rev. D* **100**, 032006 (2019).
- [26] E. Eichten, K. Gottfried, T. Kinoshita, K. D. Lane and T. M. Yan, Charmonium: The Model, *Phys. Rev. D* **17**, 3090 (1978) Erratum: [*Phys. Rev. D* **21**, 313 (1980)].
- [27] T. Barnes, S. Godfrey and E. S. Swanson, Higher charmonia, *Phys. Rev. D* **72**, 054026 (2005).
- [28] S. Godfrey, Spectroscopy of B_c mesons in the relativized quark model, *Phys. Rev. D* **70**, 054017 (2004).
- [29] S. Godfrey and K. Moats, Bottomonium Mesons and Strategies for their Observation, *Phys. Rev. D* **92**, 054034 (2015).
- [30] O. Lakhina and E. S. Swanson, A Canonical $D_s(2317)?$, *Phys. Lett. B* **650**, 159 (2007).
- [31] Q. F. L., T. T. Pan, Y. Y. Wang, E. Wang and D. M. Li, Excited bottom and bottom-strange mesons in the quark model, *Phys. Rev. D* **94**, 074012 (2016).
- [32] D. M. Li, P. F. Ji and B. Ma, The newly observed open-charm states in quark model, *Eur. Phys. J. C* **71**, 1582 (2011).
- [33] W. J. Deng, H. Liu, L. C. Gui and X. H. Zhong, Charmonium spectrum and their electromagnetic transitions with higher multipole contributions, *Phys. Rev. D* **95**, 034026 (2017).
- [34] W. J. Deng, H. Liu, L. C. Gui and X. H. Zhong, Spectrum and electromagnetic transitions of bottomonium, *Phys. Rev. D* **95**, 074002 (2017).
- [35] S. Godfrey and N. Isgur, Mesons in a Relativized Quark Model with Chromodynamics, *Phys. Rev. D* **32**, 189 (1985).
- [36] W. Roberts and M. Pervin, Heavy baryons in a quark model, *Int. J. Mod. Phys. A* **23**, 2817 (2008).
- [37] L. Y. Xiao and X. H. Zhong, Ξ baryon strong decays in a chiral quark model, *Phys. Rev. D* **87**, 094002 (2013).
- [38] E. Hiyama, Y. Kino, and M. Kamimura, Gaussian expansion method for few-body systems, *Prog. Part. Nucl. Phys.* **51**, 223 (2003).
- [39] M. S. Liu, Q. F. L., X. H. Zhong and Q. Zhao, All-heavy tetraquarks, *Phys. Rev. D* **100**, 016006 (2019).
- [40] A. Manohar and H. Georgi, Chiral Quarks and the Nonrelativistic Quark Model, *Nucl. Phys. B* **234**, 189 (1984).
- [41] Q. Zhao, J. S. Al-Khalili, Z. P. Li and R. L. Workman, Pion photoproduction on the nucleon in the quark model, *Phys. Rev. C* **65**, 065204 (2002).
- [42] Z. P. Li, The Threshold pion photoproduction of nucleons in the chiral quark model, *Phys. Rev. D* **50**, 5639 (1994).
- [43] Z. P. Li, H. X. Ye and M. H. Lu, An Unified approach to pseudoscalar meson photoproductions off nucleons in the quark model, *Phys. Rev. C* **56**, 1099 (1997).
- [44] X. H. Zhong and Q. Zhao, η' photoproduction on the nucleons in the quark model, *Phys. Rev. C* **84**, 065204 (2011).
- [45] Zhenping Li, The Kaon photoproduction of nucleons in the chiral quark model, *Phys. Rev. C* **52**, 1648 (1995).
- [46] X. H. Zhong and Q. Zhao, Strong decays of heavy-light mesons in a chiral quark model, *Phys. Rev. D* **78**, 014029 (2008).
- [47] Q. Zhao, Z. P. Li and C. Bennhold, Vector meson photoproduction with an effective Lagrangian in the quark model, *Phys. Rev. C* **58**, 2393 (1998).
- [48] X. H. Zhong, Q. Zhao, J. He and B. Saghai, Study of $\pi^- p \rightarrow \eta n$ at low energies in a chiral constituent quark model, *Phys. Rev. C* **76**, 065205 (2007).
- [49] S. J. Brodsky and J. R. Primack, The Electromagnetic Interactions of Composite Systems, *Annals Phys.* **52**, 315 (1969).
- [50] F. E. Close and L. A. Copley, Electromagnetic interactions of weakly bound composite systems, *Nucl. Phys. B* **19**, 477 (1970).
- [51] Q. Zhao, Eta-prime photoproduction near threshold, *Phys. Rev. C* **63**, 035205 (2001).
- [52] B. Saghai and Zhenping Li, Quark model study of the eta photoproduction: Evidence for a new S_{11} resonance?, *Eur. Phys. J. A* **11**, 217 (2001).
- [53] J. He, B. Saghai and Z. Li, Study of η photoproduction on the proton in a chiral constituent quark approach via one-gluon-exchange model, *Phys. Rev. C* **78**, 035204 (2008).
- [54] J. He and B. Saghai, Combined study of $\gamma p \rightarrow \eta p$ and $\pi^- p \rightarrow \eta n$ in a chiral constituent quark approach, *Phys. Rev. C* **80**, 015207 (2009).
- [55] J. He and B. Saghai, η production off the proton in a Regge-plus-chiral quark approach, *Phys. Rev. C* **82**, 035206 (2010).
- [56] X. H. Zhong and Q. Zhao, η photoproduction on the quasi-free nucleons in the chiral quark model, *Phys. Rev. C* **84**, 045207 (2011).
- [57] L. Y. Xiao, X. Cao and X. H. Zhong, Neutral pion photoproduction on the nucleon in a chiral quark model, *Phys. Rev. C*

- 92**, 035202 (2015).
- [58] E. Kaxiras, E. J. Moniz and M. Soyeur, Hyperon Radiative Decay, Phys. Rev. D **32**, 695 (1985).